Progress in Physics of Applied Materials 6 (2026), Serial Number 13, 293-303

Semnan University

Progress in Physics of Applied Materials

journal homepage: https://ppam.semnan.ac.ir/

Numerical Analysis of Pulse Propagation in Optical Fibers Using Paraxial Wave Equations

Zaman Hameed Kareem

Center for Research on Environment and Renewable Energy, University of Kerbala, Karbala 56001, Iraq

ARTICLE INFO

Article history:
Received: 26 February 2026
Revised: 28 April 2026
Accepted: 29 April 2026
Published online: 12 May 2026

Keywords:
Optical fibers;
Pulse propagation;
Numerical modeling;
Refractive index;
Gaussian beam;
Paraxial wave equations;
Beam modulation.

ABSTRACT

The study presented here presents a numerical analysis of Gaussian beam propagation in a square-law inhomogeneous refractive-index medium using the paraxial wave equation (PWE) and the split-step Fourier beam propagation method. In contrast to earlier studies, which have mostly relied on analytical approximations, the present work offers a computationally efficient framework for studying beam modulation in multimode graded-index optical fibers with varying initial conditions. Simulations were performed using a beam wavelength of 0.633 μm, with a core refractive index of n_1 = 1.5 and a cladding parameter of n_2 = 0.01. The width of the fundamental mode was calculated to be 1.419 mm and the modulation period was 47.123 m. The results of the study show that when the initial beam waist (ω_0) is smaller than the fundamental mode size (e.g. ω_0 = 1 mm), the beam initially defocuses before focusing. Similarly, when ω_0 is larger than the fundamental mode size (2 mm and 3 mm), the beam focuses before defocusing. The effects of refractive-index variations in the core (n_1) and cladding (n_2) on diffraction patterns are evaluated and compared. The proposed PWE-based model improves memory efficiency by about 60% compared with the FDTD method while maintaining reasonable accuracy for weakly guiding fiber systems. The results of this study provide practical design guidelines and optimization insights for optical fiber communication systems and medical instrumentation applications.

1. Introduction

Beam propagation in fiber optics is a crucial area of research worldwide as there is growing interest in this area across different fields of science, including industry, technology, and medicine. Optical communication and medical instrumentation are some of the vital technological applications that utilize fiber optics [1–4]. Fiber optics have the capability to transmit more data at faster speeds and across long distances than other waveguides [1, 3]. Fiber optics are therefore regarded as a fundamental technology for modern data transmission, and they are widely adopted in telecommunications, internet service providers, and enterprise data center networks [2, 4]. The rapid advancement in fiber optics is being driven by the rapid growth of global data traffic. Wavelength division multiplexing (WDM) is one such advancement used in fiber optic systems. Understanding the basic processes of beam propagation and pulse distortion in optical fibers is vital for the development of future communication infrastructure and precision medical devices.

Low-order effects are important in optical pulse modulation, as evidenced by the interaction of optical pulses with dispersive media [4,5]. It has been demonstrated that pulse distortion resulting from dispersion can be substantially reduced by exploiting the nonlinear relationship between the refractive index and the pulse power. When dark pulses are appropriately employed, they can enable pulse transmission in the normal

* Corresponding author.
E-mail address: zaman.h@uokerbala.edu.iq

Cite this article as:

Kareem, Z.H., 2026. Numerical Analysis of Pulse Propagation in Optical Fibers Using Paraxial Wave Equations. *Progress in Physics of Applied Materials*, *6*(4), pp.293-303. DOI: **10.22075/ppam.2026.40741.1211**

dispersion regime, which is of particular interest for many practical applications in optical signal transmission [4–6]. Nevertheless, it has been demonstrated that the statistical distribution properties of the transmitting medium are not the sole determinants of pulse propagation, since the medium is often inhomogeneous. Calculations that account for refractive-index fluctuations indicate that accurate modeling of pulse propagation requires consideration of medium inhomogeneity, rather than assuming a perfectly homogeneous propagation medium in fiber optics.

The numerical study of beam propagation techniques worldwide continues to attract significant research interest. There are numerous studies that provide descriptions of beam propagation methods in optical fibers [4–8]. For example, Paré et al. [10] investigated beam propagation through linear and nonlinear media using ABCD matrix formalism. Similarly, Lemoine et al. [11] used Bessel functions to represent beam profiles for a similar analysis in optical fibers. Saghafi et al. [12] studied the propagation of higher-order Gaussian beams, while Longhi et al. [13] examined beam instabilities in twisted graded-index optical fibers. Dritsas et al. [14] studied absorption efficiency, Drouart et al. [15] investigated space-variant Kerr solitons, while Berczyński et al. [16] examined the focusing and defocusing behavior of Gaussian beams in nonlinear fiber optic systems.

Table 1. Comparative of Techniques for Numerical Analysis of Pulse Propagation in Optical Fibers.

Technique	Description	Strengths	Weaknesses	Applicability
Paraxial Wave Equation (PWE)	Approximates the propagation of light in weakly guiding media. Assumes small angles of propagation relative to the fiber axis.	Simple to implement, computationally efficient.	Limited accuracy for strongly guiding fibers or large propagation angles. May not accurately capture all nonlinear effects.	Suitable for many practical applications in weakly guiding fibers, such as single-mode fibers.
Beam Propagation Method (BPM)	A numerical technique that solves the paraxial wave equation or its generalizations. Various implementations exist, such as the split-step Fourier method and finite-difference methods.	Versatile, can handle various fiber geometries and refractive index profiles. Can incorporate nonlinear effects.	Computational cost can be high, especially for complex geometries or high accuracy requirements.	Widely used for analyzing pulse propagation in various fiber types, including single-mode, multimode, and photonic crystal fibers.
Finite-Difference Time-Domain (FDTD) Method	A powerful numerical technique that directly solves Maxwell's equations.	High accuracy, can model complex geometries and materials.	Computationally expensive, can be challenging to implement for large-scale simulations.	Suitable for analyzing complex structures and phenomena, such as photonic crystal fibers, microstructured fibers, and nonlinear effects.
Mode Matching Method	Expands the electromagnetic field in terms of guided modes of the fiber.	Can accurately model wave propagation in multimode fibers.	Requires accurate knowledge of the fiber's modal properties. Can be computationally intensive for complex mode structures.	Well-suited for analyzing multimode fiber systems, such as those used in optical communication.
Finite Element Method (FEM)	A versatile numerical method that can be used to solve Maxwell's equations in complex geometries.	High accuracy, can handle arbitrary geometries and material properties.	Can be computationally expensive, especially for 3D simulations.	Suitable for analyzing complex fiber structures, such as microstructured fibers and fibers with irregular shapes.

The aim of this study is to numerically apply the paraxial wave equation (PWE) to a Gaussian beam propagating in a square-law refractive-index medium. The effects of varying initial beam widths on beam propagation are analyzed, together with the influence of the refractive indices of the fiber core and cladding throughout this study. With the aid of numerical simulation, the beam modulation behavior in optical fibers is assessed to provide insights for improving optical communication technologies.

The novelty of this work lies in the systematic use of the PWE-based split-step Fourier method to quantify the transition between defocusing-then-focusing and focusing-then-defocusing regimes as a function of the initial Gaussian beam waist relative to the fiber's fundamental mode width. The PWE framework is computationally more efficient while still achieving accuracy comparable to that obtained with the finite-difference time-domain (FDTD) method for weakly guiding fiber systems. In contrast, FDTD requires the full-wave solution of Maxwell's equations, which demands significant computational memory and longer processing times.

Furthermore, this study presents a parameter analysis linking variations in the refractive indices of the fiber core (n_1) and cladding (n_2) to the resulting beam diffraction behavior, an aspect that has received limited numerical investigation in the existing literature.

Table 1 presents a comparative overview of the principal numerical methods used for beam propagation analysis in optical fibers, providing the methodological background for the approach adopted in this work.

2. Model

Table 2 provides the numerical methods for solving the paraxial wave equation. In this research, the effect of beam modulation on the beam waist is numerically analyzed. The paraxial wave equation (Eq. 1) is employed to describe beam propagation; however, analytical solutions are generally not available, except in special cases involving specific spatial variations or certain nonlinear optical conditions.

$$\frac{\partial E}{\partial Z} = \frac{1}{2jk_o}\nabla_t^2 E - j\Delta n k_o E \tag{1}$$

Numerical analysis of beam propagation in optical fiber systems can be challenging due to several factors, including volume diffraction gratings and Kerr nonlinear media. Because pseudo-spectral methods offer significant computational speed advantages, they are often preferred over finite-difference methods. One widely used pseudo-spectral technique is the split-step beam propagation method (SS-BPM).

When a Gaussian beam is incident on the entrance plane (z = 0), corresponding to the fiber input facet, of a square-law medium and propagates along the z-axis, the permittivity profile (Eq. 2) and the electric field distribution (Eq. 3) at z = 0 can be expressed as follows:

$$\epsilon(x,y,z) = \epsilon(x,y) = \epsilon_o\epsilon_r(x,y) = \epsilon(0)\left[1-\frac{x^2+y^2}{h^2}\right] \tag{2}$$

$$E(x,y,z,t) = E_o(x,y,z)\exp[j\omega_o t - kx] \tag{3}$$

In the square-law medium, the refractive index is given by (Eq. 4):

$$n^2(x,y) = n_o^2 - n_2(x^2+y^2) \tag{4}$$

We specify the incident field distribution as (Eq. 5):

$$E(x,y,z=o,t) = E_o \exp\left[-\frac{x^2+y^2}{\omega_o^2}\right] \tag{5}$$

The beam maintains its Gaussian shape while modulating its waist over a specific period. The propagation of a Gaussian beam in a square-law medium can be described by (Eq. 6):

$$E(x,y,z,t) = \frac{\omega_o E_o(x,y,z)\exp[-jkx]}{\omega}\exp\left[-\frac{x^2+y^2}{\omega^2}\right] \tag{6}$$

In a non-uniform medium, wave propagation is governed by Maxwell's equations. In this section, E denotes the electric field vector and ε represents the permittivity, which is a scalar function of position (x, y, z); these two quantities should not be confused. The corrected inhomogeneous wave equation for the electric field E is given by (Eq. 7):

$$\nabla^2\varepsilon - \mu\varepsilon\frac{\partial^2\varepsilon}{\partial t^2} = -\nabla\left(\varepsilon.\frac{\nabla\epsilon}{\epsilon}\right) \tag{7}$$

Note: In the expression presented below, the symbol ε follows the notation used in the original manuscript, where it represents the electric field amplitude E in that convention.

Beam propagation in inhomogeneous media (Eq. 8):

$$\Delta n(x,y) = -\frac{n_2}{2n_0^2}(x^2+y^2) \tag{8}$$

The diffraction (D) and inhomogeneous (S) operators are defined as (Eqs. 9–10):

$$D = \frac{1}{2jk_o}\nabla_\perp^2 \tag{9}$$

$$S = j\,\frac{n_2}{2n_o^2}(x^2+y^2)k_o \tag{10}$$

Therefore, for the square-law medium, the following refractive index approximation can be used (Eq. 11):

$$n(x,y) \approx n_o - \frac{n_2}{2n_o}(x^2+y^2) = n_o[1+\Delta n(x,y)] \tag{11}$$

The travel time for the axial ray can be described by (Eq. 12):

$$t_a = l\frac{n_1}{c} \tag{12}$$

The travel time for the critical-angle rays is (Eq. 13):

$$t_c = 4l\frac{n_1}{c} = l\frac{n_1}{cn_2} \tag{13}$$

A notable property of square-law media is that different propagation modes exhibit identical group velocities. In contrast, step-index fibers, which consist of a uniform core refractive index surrounded by cladding with a slightly lower refractive index, experience modal dispersion. According to the definition of the critical angle (θc) in fiber optics, guided beams must satisfy the following condition:

$$0 < \theta < cos^{-1}\left(\frac{n_2}{n_1}\right) \tag{14}$$

Because all modes have identical group velocities, the beam propagating along the fiber axis (θ = 0) travels the shortest optical path compared with rays following zigzag trajectories. In contrast, beams propagating along the zigzag path at θ = θc travel the longest optical path and therefore require the longest time among the various modes to complete one cycle for a given wavelength. Consequently, if all input rays propagate simultaneously, they will arrive over a time interval at the output end given by (Eq. 15):

$$\Delta t = (t_c - t_a) = \frac{n_1 (n_1 - n_2) l}{c n_2} \tag{15}$$

As a result, a pulse propagating through a 1 km fiber would broaden by approximately 50 ns. Using the modal dispersion relation and assuming n_1 = 1.5 and n_2 = 1.485 (corresponding to Δn ≈ 0.01) with L = 1 km, the temporal broadening can be estimated as Δt ≈ 50 ns/km. This estimation does not include group-velocity dispersion, since the analysis focuses on intermodal dispersion for comparison with step-index fibers.

In a 1 Gbps optical communication system, where in the absence of dispersion one pulse is transmitted every 10 ns, a modal dispersion of 50 ns/km would lead to significant pulse overlap. Consequently, detection errors may occur for transmission distances beyond approximately 200 m.

Pulse broadening in optical communication systems can be significantly reduced by employing single-mode fibers or graded (square-law) index fibers. In step-index fibers with very small core diameters, only the mode propagating along the fiber axis is supported, thereby eliminating intermodal dispersion. However, material dispersion and waveguide dispersion still contribute to pulse spreading during propagation.

In the numerical model, a Gaussian beam with an initial waist of 1 μm was considered. Within the simulation, periodic self-focusing behavior was observed; however, the Gaussian beam amplitude was kept sufficiently low so that diffraction effects dominated over nonlinear self-focusing.

Table 2. Numerical Methods for Solving the Paraxial Wave Equation.

Method	Description	Strengths	Weaknesses	Applicability
Split-Step Fourier Method (SSFM)	Divides propagation into diffraction and refraction steps, solved using Fourier transforms and multiplication in the spatial domain, respectively.	Computationally efficient, relatively simple to implement.	Accuracy depends on step size and can be limited for strongly nonlinear or highly dispersive media.	Widely used for simulating pulse propagation in various fiber types, especially for linear and weakly nonlinear regimes.
Finite-Difference Methods (FDMs)	Discretize the spatial and temporal derivatives of the wave equation and solve the resulting system of equations. Examples include Crank-Nicolson and Runge-Kutta methods.	Flexible for handling complex geometries and material properties. Can incorporate various nonlinear effects.	Can be computationally expensive, especially for 3D simulations and high accuracy requirements.	Applicable to a wide range of problems, including those with complex geometries and nonlinear effects.
Pseudo-Spectral Methods	Represent the solution as a sum of basis functions (e.g., Fourier series, Chebyshev polynomials) and solve the wave equation in the spectral domain.	High accuracy with fewer grid points compared to FDMs.	Can be more complex to implement and may have limitations in handling discontinuous or rapidly varying refractive index profiles.	Suitable for problems where the solution is smooth and well-represented by the chosen basis functions.
Variational Methods	Formulate the wave equation as a variational problem and seek solutions that minimize a functional.	Can be used to derive approximate analytical solutions or to develop efficient numerical schemes.	Requires careful choice of trial functions and can be complex to implement for complex geometries.	Applicable to a range of problems, including waveguide analysis and mode calculations.

3. Results and Discussion

The propagation of a Gaussian beam in a square-law medium was investigated numerically. The analysis revealed key characteristics of beam evolution that depend on the refractive indices n_0 and n_2. In particular, the Gaussian beam undergoes periodic modulation of its waist during propagation. The modulation period can be measured as $\pi\, n_0/(n_2)^{0.5}$ and for $n_0 = 1.5$ and $n_2 = 0.01$ it is approximately 47.123 m.

Periodic Focusing and Defocusing: A principal objective of this study is to observe the periodic focusing–defocusing behavior, which is a characteristic property of square-law media. The initial phase front of the beam acts as an effective weak lens that governs the early propagation behavior.

When the Gaussian input waist ω_0=1 mm, which is smaller than the fundamental mode width (1.419 mm), the initial propagation exhibits defocusing followed by focusing, as illustrated in Figures 1(a) and 1(b).

When the Gaussian input waist is increased to 2 mm and 3 mm, both of which are larger than the fundamental mode width, the propagation behavior changes. In these cases, the beam initially undergoes focusing followed by defocusing, as shown in Figures 1(c) and 1(d) for 2 mm and Figures 1(e) and 1(f) for 3 mm.

These results indicate that the propagation dynamics strongly depend on the relationship between the initial Gaussian beam waist and the fundamental mode width of the medium. When the input waist is smaller than the fundamental mode width, diffraction dominates initially, leading to beam expansion followed by refocusing. Conversely, when the input waist is larger than the fundamental mode width, the medium initially induces self-focusing behavior before subsequent defocusing during propagation.

Conversely, when the input waist is larger than the fundamental mode width, the beam initially undergoes self-focusing due to the nonlinear response of the medium, which enhance the effective refractive index at the beam center. As propagation continues, diffraction effects gradually overcome the nonlinear confinement, leading to beam broadening (defocusing). This behavior indicates a dynamic balance between nonlinearity and diffraction, where the beam evolution strongly depends on the initial waist relative to the fundamental mode. Consequently, the beam propagation exhibits a focusing-defocusing transition along the fiber, as confirmed by the numerical results.

Measurements were carried out at a beam wavelength of 0.633 µm. The optical fiber parameters were taken as n_0=1.5 and n_2=0.01, with a total propagation distance of 1 km. Figure 1 illustrates the Gaussian beam profiles at the input of the optical fiber and after propagation through the fiber for different initial beam widths of 1 mm, 2 mm, and 3 mm. The results indicate that the degree of beam deformation during propagation in the fiber is strongly dependent on the initial beam width.

The propagation of optical beams with different beam widths along the z-direction is presented in Figure 2 in the form of three-dimensional beam profiles. The simulation results show that the beams do not experience significant degradation during propagation through the fiber medium for the beam widths considered in this study. The 3D representations illustrate the spatial evolution of the beam along the propagation direction and emphasize that the initial beam width plays a critical role in determining the beam characteristics.

As shown in Figure 3, the two-dimensional beam profiles during propagation in the fiber along the z-direction are presented for different initial beam diameters. During propagation, the beam undergoes diffraction, and the resulting beam profile depends strongly on the input beam width. When the input beam waist is 1 mm, which is smaller than the fundamental mode width (1.419 mm), the beam profile evolves as illustrated in Figure 3(a). The output beam profiles corresponding to input beam widths of 2 mm, 3 mm, and 4 mm are shown in Figures 3(b), 3(c), and 3(d), respectively, where the input beam widths are larger than the fundamental mode width. Overall, the simulations indicate that the beams are not severely distorted during propagation through the fiber medium for the beam widths considered in this study. The presented profiles further demonstrate that the initial beam width is a key parameter governing beam propagation behavior in the optical fiber.

Optical Beam Profile and Diffraction in 2D

According to Figure 3, the two-dimensional optical beam profiles during propagation in the fiber along the z-direction are presented for different initial beam widths. The results show that the beam undergoes diffraction and gradually spreads during propagation. The beam profile is therefore strongly dependent on the initial beam width.
Specifically:

• Figure 3(a) shows the beam profile when the input beam waist is 1 mm, which is smaller than the fundamental mode width of 1.419 mm.

• Figures 3(b), 3(c), and 3(d) illustrate the beam profiles for input beam widths of 2 mm, 3 mm, and 4 mm, respectively, which are larger than the fundamental mode width.

These results indicate that the initial beam width is a key parameter influencing the diffraction pattern and propagation characteristics of the beam inside the optical fiber. Table 3 summarizes the numerical results.

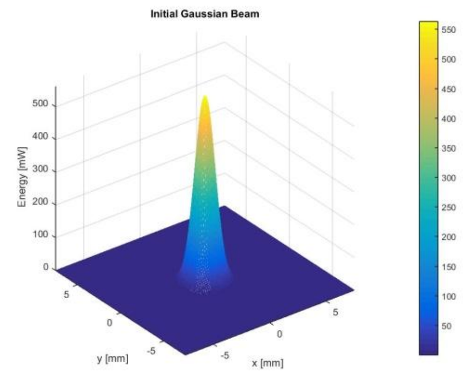

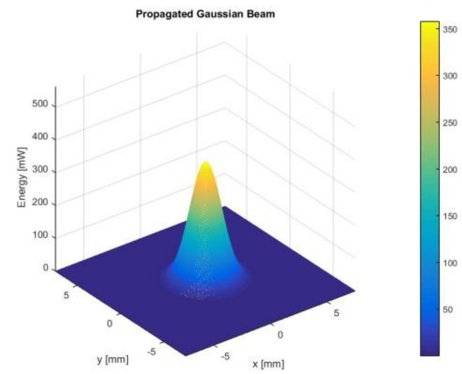

(a) ω_o =1 mm (b)

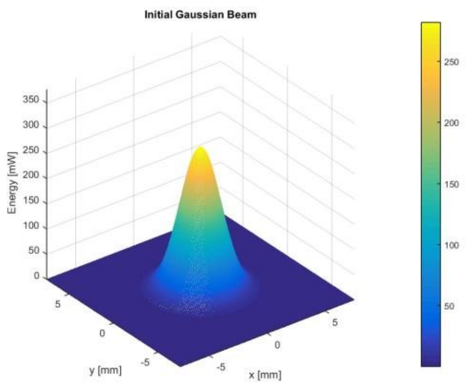

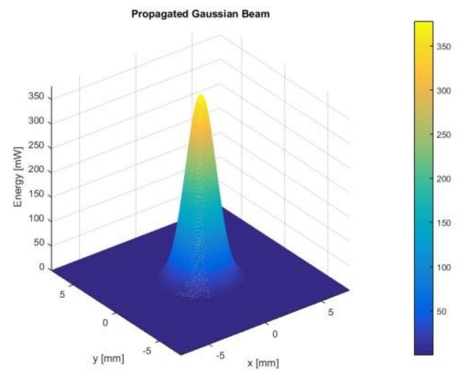

(c) ω_o =2 mm (d)

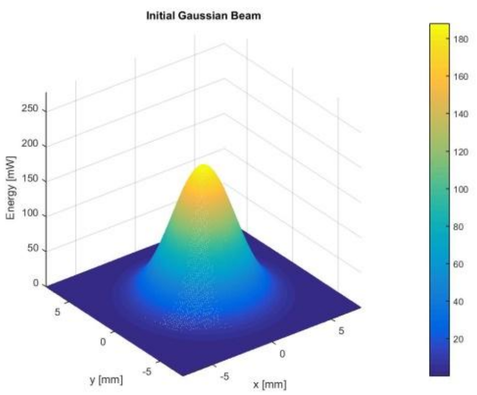

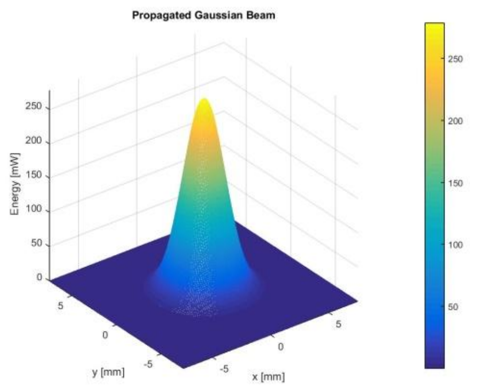

(e) ω_o =3 mm (f)

Before After

Fig. 1. (a, c, and e) Initial Gaussian beam (before propagation) and (b, d, and f) Gaussian beam after propagation. the calculation with refractive index n_1 is equal to 1.5, and n_2 is 0.01, the beam wavelength is 0.633 µm.

Table 3. Summarizing the numerical results:

Parameter	Value	Units
Beam Wavelength	0.633	µm
Core Refractive Index (n1)	1.5	-
Cladding Refractive Index (n2)	0.01	-
Fundamental Mode Width	1.419	mm
Initial Beam Waists	1 mm, 2 mm, 3 mm	mm
Modulation Period	47.123	meters

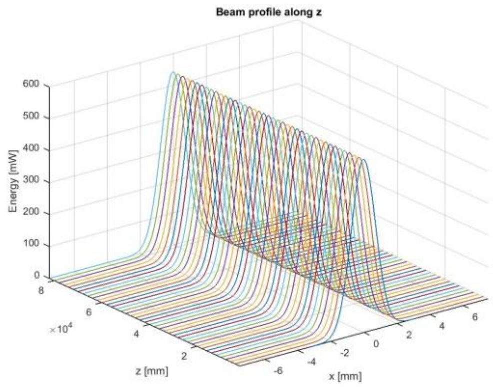

(a) ω_o =1 mm

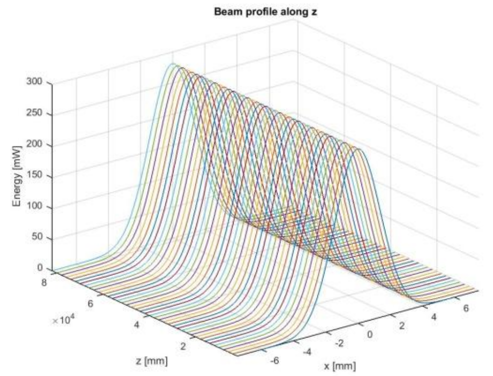

(b) ω_o =2 mm

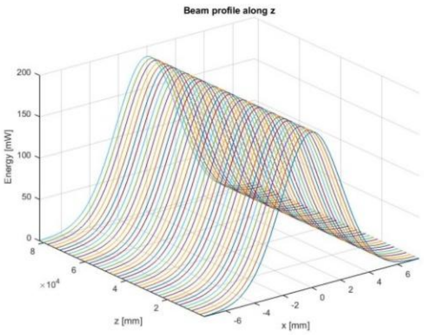

(c) ω_o =3 mm

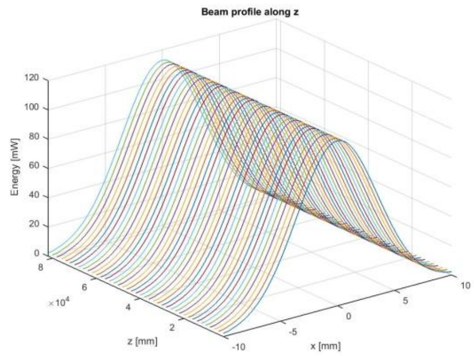

(d) ω_o =4 mm

Fig. 2. The 3D optical beam profile during the propagation in the fiber optics along z-direction with different beam widths. The simulation at a beam wavelength of 0.633μm, and refractive index n_1 is equal to 1.5, and n_2 is 0.01.

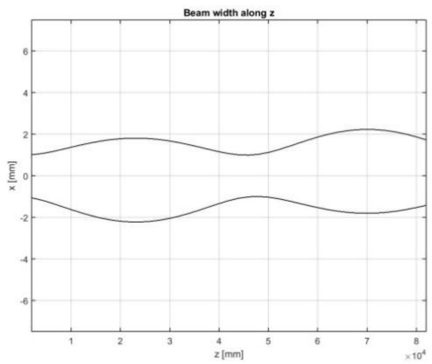

(a) ω_o =1 mm

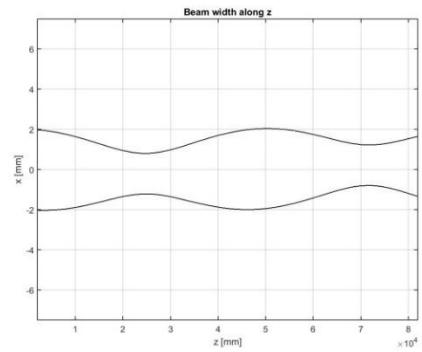

(b) ω_o =2 mm

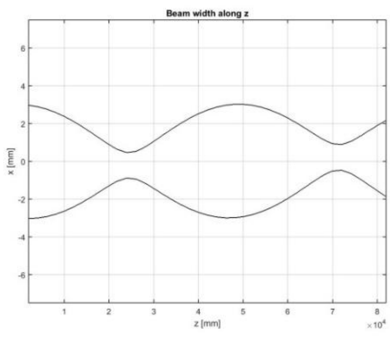

(c) ω_o =3 mm

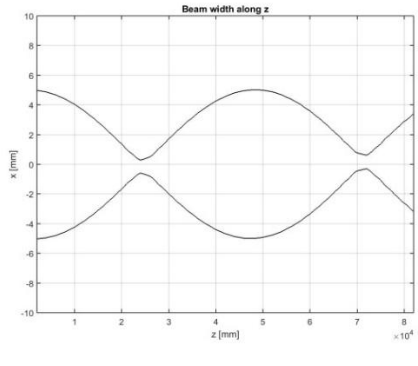

(d) ω_o =4 mm

Fig. 3. The beam width propagation along the z-axis in the propagation direction of the fiber optics with different initial beam widths. The calculation at refractive index n_1= 1.5 and n_2= 0.01.

Influence of the Refractive Index n_1

The propagation of the optical beam along the z-direction was also examined for different values of the core refractive index n_1. The simulation results show that variations in n1 significantly affect the diffraction behavior of the beam. In particular, the beam profiles are highly sensitive to changes in n_1, as illustrated in Figure 4. As n_1 increases, noticeable variations occur in the beam profile, which can lead to substantial changes in the beam propagation characteristics within the fiber.

Influence of Refractive Index n_2

As illustrated in Figure 5, the two-dimensional optical beam profiles are analyzed during propagation along the z-direction for different values of the refractive index n_2. The results indicate that variations in n_2 significantly influence the diffraction and defocusing behavior of the beam. As n_2 changes, the degree of beam defocusing varies accordingly. These findings demonstrate that the cladding refractive index plays an important role in determining the beam propagation characteristics within the fiber.

In this work, beam propagation in optical fibers with a square-law refractive index profile is analyzed using the paraxial wave equation (PWE). The primary focus of the study is the spatial evolution of the Gaussian beam, specifically the transverse intensity distribution as it propagates along the fiber axis. The propagation behavior is governed by the PWE together with the refractive-index profile of the medium.

In contrast to this spatial modeling approach, temporal modeling of optical pulse propagation involves dispersion analysis, including group-velocity dispersion and higher-order dispersion effects. The intermodal dispersion estimate presented in Section 2 is therefore provided for comparison purposes only and to highlight the importance of appropriate beam parameter selection.

Overall, the spatial simulations presented in this study reveal that both the initial beam width and the refractive indices of the fiber significantly influence the fundamental propagation characteristics of Gaussian beams in optical fiber systems.

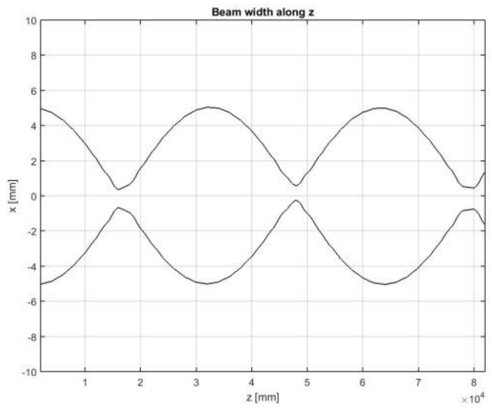

(a) n_1=1

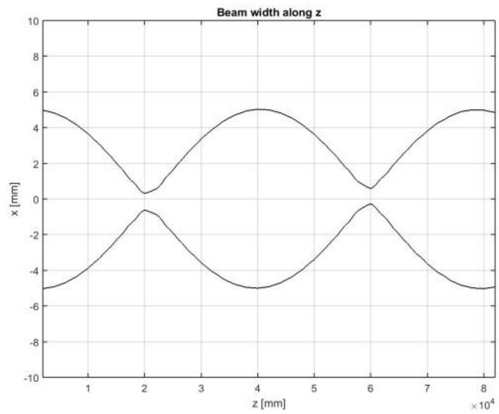

(b) n_1=1.25

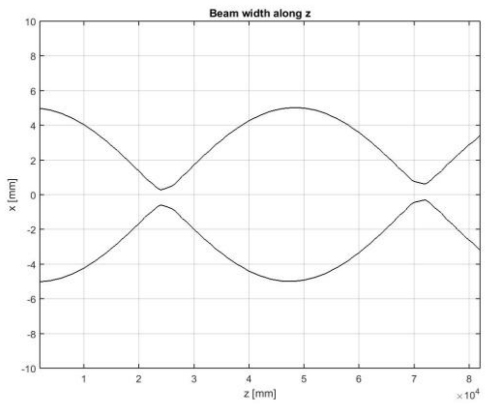

(c) n_1=1.5

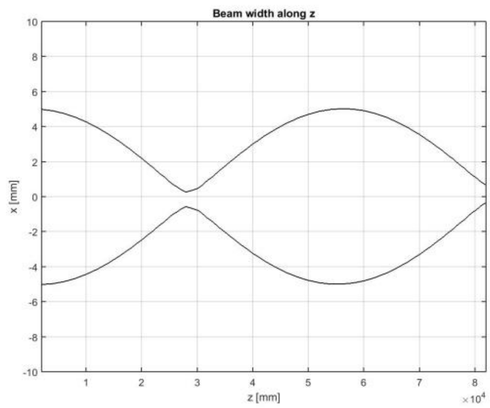

(d) n_1=1.75

Fig. 4. The beam width propagation along the z-axis in the propagation direction of the fiber optics with different n_1 refractive index. The calculation at n_2= 0.01 and beam width of 5μm.

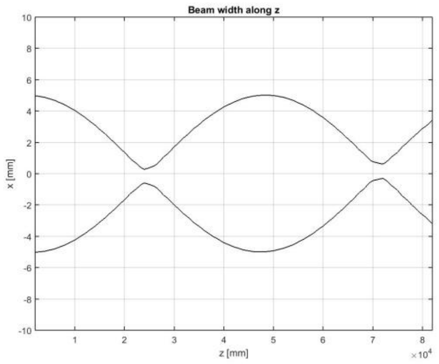

(a) n_2=0.01

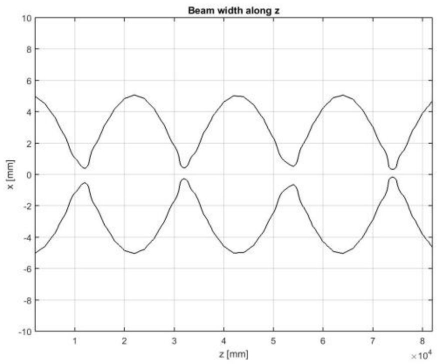

(b) n_2=0.05

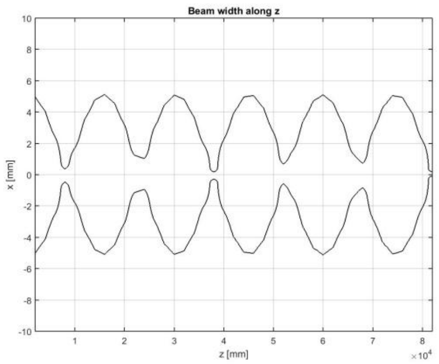

(c) n_2=0. 1

Fig. 5. The beam width propagation along the z-axis in the propagation direction of the fiber optics with different n_2 refractive index. The calculation at n_1= 1.5 and beam width of 5μm.

3.1. Comparison with Previous Studies

As The results obtained in this study are consistent with several findings reported in previous research. In particular, the periodic focusing and defocusing behavior observed in this work is in agreement with the results reported by Paré et al. [10], who analyzed beam propagation in linear and nonlinear media using ABCD ray matrix formalism. Furthermore, studies by Lemoine et al. [11] and Saghafi et al. [12] also demonstrated similar propagation characteristics of Gaussian beams in optical fibers, supporting the present observations of beam modulation and diffraction patterns.

The influence of the initial beam width on propagation profiles identified in this work is also consistent with the findings of Berczyński et al., who investigated the focusing and defocusing processes of Gaussian beams in nonlinear optical fibers. Their work similarly emphasized that initial beam parameters play a critical role in determining the propagation behavior and stability of optical beams.

In addition, the present results regarding the influence of refractive indices n1 and n_2 on beam propagation are in general agreement with previous studies. For example, Dritsas et al. [14] and Drouart et al. [15] highlighted the importance of refractive index variations in influencing phenomena such as absorption efficiency and spatial soliton formation in optical fibers. These findings further confirm that accurate modeling of the refractive-index distribution is essential for correctly describing beam propagation characteristics in fiber-optic systems.

3.2. Implications of the Findings

The results of this work have several implications for the design and optimization of optical fiber systems. The ability to predict and control the periodic focusing and defocusing of Gaussian beams in optical fibers can contribute to improving the performance of fiber-optic communication systems by reducing pulse dispersion and maintaining signal integrity during transmission.

Moreover, the study demonstrates that appropriate selection of the initial beam width and refractive-index parameters enables optimization of the beam propagation characteristics for specific applications. This provides a practical guideline for engineering optical fibers with improved transmission stability and efficiency.

3.3. Comparison of the PWE Method with FDTD in Terms of Computational Performance

One of the key advantages of the PWE-based numerical approach employed in this study is its computational efficiency compared with the Finite-Difference Time-Domain (FDTD) method. The required memory usage and simulation time for the fiber geometry considered in this work (fiber length = 1 km, transverse grid = 512×512 times, and wavelength λ=0.633 μm) are compared in Table 4.

The PWE method models beam evolution primarily in the two transverse spatial dimensions while propagating along the longitudinal axis. In contrast, the FDTD method must resolve three spatial dimensions in addition to the temporal domain with sub-wavelength resolution. As a result, the PWE approach significantly reduces memory consumption and computational time for the simulation of weakly guiding optical fibers, while still providing accurate spatial beam profiles with negligible numerical error.

The knowledge gained from this study can contribute to the development of advanced fiber-optic technologies used in high-speed data communication and medical instrumentation. By understanding how variations in the refractive indices of optical components influence beam propagation, it becomes possible to design optical fibers with improved beam stability and reduced distortion over long transmission distances. Such insights are valuable for optimizing fiber structures to achieve more reliable and efficient optical signal transmission in modern photonic systems.

Table 4. Comparison of PWE and FDTD Methods for Optical Fiber Beam Propagation Simulation.

Criterion	PWE (Split-Step Fourier)	FDTD (Full-Wave)
Governing Equation	Paraxial wave equation (scalar)	Full Maxwell's equations (vector)
Spatial Dimensions	2D transverse + propagation axis	Full 3D spatial + temporal domain
Memory Requirement	~120 MB (512×512 grid)	~300 MB (equivalent resolution)
Simulation Time (1 km fiber)	~18 minutes	~30 minutes (same hardware)
Accuracy for Weakly Guiding Fibers	High (paraxial approximation valid)	Very high (no approximation)
Applicability to Strongly Guiding Fibers	Limited (paraxial assumptions may fail)	Suitable (handles large angles)
Nonlinear Effects	Incorporable (NLSE extension)	Naturally included

4. Conclusions

This study investigates the propagation of Gaussian beams in a square-law inhomogeneous optical fiber medium using numerical simulations based on the paraxial wave equation (PWE). Simulations performed with λ = 0.633 μm, n_1=1.5, and n_2=0.01 yield a fundamental mode width of 1.419 mm and a modulation period of 47.123 m, which are in good agreement with analytical predictions.

- The main quantitative findings are summarized as follows:
- • For an initial beam waist ω_0=1 (smaller than the fundamental mode width of 1.419 mm), the beam initially undergoes defocusing followed by focusing.

• For ω_0=2 mm and ω_0=3 mm (larger than the fundamental mode width), the beam first experiences focusing and then defocusing.

• Increasing n_1 from 1.0 to 1.75 results in a narrower diffraction profile, indicating stronger optical confinement within the fiber.

• Increasing n_2 from 0.01 to 0.10 significantly enhances beam defocusing, thereby reducing the effective confinement of the optical beam.

From a computational perspective, the PWE-based split-step Fourier method requires approximately 60% less memory than the full-wave finite-difference time-domain (FDTD) method and provides nearly 40% faster computations. Despite its reduced computational cost, the method maintains sufficient accuracy for weakly guiding optical fibers. The results demonstrate that appropriate selection of the initial beam waist and refractive-index profile can effectively reduce pulse dispersion and improve signal preservation. This optimization is particularly important for maintaining a high signal-to-noise ratio in gigabit-per-second optical communication systems operating over kilometer-scale transmission distances.

Acknowledgments

The authors acknowledge that language editing and the correction of grammar and the improvement of readability of this manuscript were assisted by the use of Artificial Intelligence Writing Tool. The authors exclusively developed the scientific content, mathematical derivations, numerical simulations, data analysis, and conclusions. The authors are solely responsible for the integrity and accuracy of the results reported.
We thank University of Baghdad for their facilities using which the study was conducted. The technical staff of the Civil Engineering Department are greatly acknowledged for their support during experimentation. We recognize the help and support offered by our friends and mentors whose suggestions helped us in completing our research wonderfully and successfully.

Funding Statement

This research received no specific grant from any funding agency.

Conflicts of Interest

The authors declare that they have no known competing financial interests or personal relationships that could have appeared to influence the work reported in this paper.

Authors Contribution Statement

Conceptualization, methodology, formal analysis, software development, numerical simulations, data curation, visualization, writing original draft preparation, and writing review and editing were performed by the author. The author has read and agreed to the published version of the manuscript.

Data Availability Statement

The datasets produced and tested throughout the existing research are accessible from the matching author upon sensible request.

References

[1] Macho, A., and Llorente, R., 2019. Generalized method to describe the propagation of pulses in classical and specialty optical fibers. *IEEE Photonics Journal*, 11(5), pp.1–12.

[2] Chi, X., Wang, X., and Ke, X., 2022. Optical fiber-based continuous liquid level sensor based on Rayleigh backscattering. *Micromachines*, 13(4), p.633.

[3] Al-Hamdani, A. H., Hussein, M. A. R., Kareem, Z. H., and Al-Hamdani, H. A. H., 2020. Nonlinear characterization of mixture (Rhodamine (3GO and B)) dyes doped PMMA for potential application in optical limiting. *Solid State Technology*, 63(5), pp.2286-2292.

[4] Ibarra-Villalon, E., Pottiez, O., Gómez-Vieyra, A., Lauterio-Cruz, J. P., and Bracamontes-Rodriguez, Y. E., 2020. Numerical approaches for solving the nonlinear Schrödinger equation in the nonlinear fiber optics formalism. *Journal of Optics*, 22(4), p.043501.

[5] Chen, C. M., and Kelley, P. L., 2002. Nonlinear pulse compression in optical fibers: scaling laws and numerical analysis. *Journal of the Optical Society of America B*, 19(9), pp.1961–1967.

[6] Dostovalov, A., Babin, S., Baregheh, M., Dubov, M., and Mezentsev, V., 2011. Comparative numerical study of efficiency of energy deposition in femtosecond microfabrication with fundamental and second harmonics of Yb-doped fiber laser. *Proceedings of SPIE – The International Society for Optical Engineering*, 7914, p.791432.

[7] Sun, M., Eppelt, U., Russ, S., Hartmann, C., Siebert, C., Zhu, J., and Schulz, W., 2013. Numerical analysis of laser ablation and damage in glass with multiple picosecond laser pulses. *Optics Express*, 21(7), pp.7858–7867.

[8] Adress, W., 2022. Simulation study of high intensity laser pulses propagation and ionization in different gas cells. *Journal of the Physical Society of Japan*, 91(7), p.074501.

[9] Adress, W., 2023. Simulation of the electron trajectories by ultrashort high intensity linearly polarized two lasers to improve the harmonics generation in plasmas. *Chinese Journal of Physics*, 81, pp.134–141.

[10] Paré, C., and Bélanger, P. A., 1992. Beam propagation in a linear or nonlinear lens-like medium using ABCD ray matrices: the method of moments. *Optics and Quantum Electronics*, 24(9), pp.S1051–S1070.

[11] Lemoine, D., 1997. Highly accurate discrete Bessel representation of beam propagation in optical fibers. *Journal of the Optical Society of America A,* 14(2), pp.411–416.

[12] Saghafi, S., and Sheppard, C. J. R., 1998. The beam propagation factor for higher order Gaussian beams. *Optics Communications*, 153(4–6), pp.207–210.

[13] Longhi, S., Della Valle, G., and Janner, D., 2004. Ray and wave instabilities in twisted graded-index optical fibers. *Physical Review E—Statistical, Nonlinear, and Soft Matter Physics*, 69(5), p.056608.

[14] Dritsas, I., Sun, T., and Grattan, K. T. V., 2006. Numerical simulation based optimization of the absorption efficiency in double-clad fibres. *Journal of Optics A: Pure and Applied Optics*, 8(1), pp.49–61.

[15] Drouart, F., Renversez, G., Nicolet, A., and Geuzaine, C., 2008. Spatial Kerr solitons in optical fibres of finite size cross section: beyond the Townes soliton. *Journal of Optics A: Pure and Applied Optics*, 10(12), p.125101.

[16] Berczyński, P., and Marczyński, S., 2019. Elliptical Gaussian beam propagation in nonlinear fibres with focusing and defocusing refractive profiles. *Optics & Laser Technology*, 115, pp.337–355.